Pergamon

Tetrahedron 55 (1999) 3767–3778

TETRAHEDRON

A He(I) Ultraviolet Photoelectron Spectroscopic and Computational Study of the Electronic Structure of Phenyl and Pyridinyl Diazoketones and Diazoesters

Heidi M. Muchall* and Nick H. Werstiuk*

Department of Chemistry, McMaster University, Hamilton, Ontario, L8S 4M1, Canada

Jason L. Pitters and Mark S. Workentin

Department of Chemistry, University of Western Ontario, London, Ontario, N6A 5B7, Canada

Received 1 June 1998; revised 28 July 1998; accepted 29 July 1998

Abstract: The He(I) photoelectron spectra of five phenyl and pyridinyl diazoketones and diazoesters **2a**, **2b**, **3**, **4a**, and **4b** have been recorded and their structures and orbital energies have been calculated by *ab initio* methods. Diazoesters **3**, **4a**, and **4b** show a π–π orbital interaction between a π orbital of the aromatic ring and $\pi_{C=N}$ of the diazo moiety which causes a dependence of orbital energies on the C=C–C=N torsional angle. Diazoketones **1**, **2a**, and **2b** do not exhibit π–π interaction as low-lying occupied molecular orbitals of the keto group function as an insulator. © 1999 Elsevier Science Ltd. All rights reserved.

INTRODUCTION

The magnitude of orbital interactions is controlled by their symmetries and energies as well as their relative orientation, i.e. when symmetries and energies of two orbitals match, the extent to which they interact will depend on the molecular conformation. Photoelectron (PE) spectroscopy, the technique of choice whenever information about bonding in organic molecules is wanted, has been employed extensively for the detection and analysis of various kinds of orbital interaction.[1] Interactions of the π–π type have been among the first studied,[1] and while there has been interest in the influence of heteroatoms in π bonds,[1] systems involving a diazoketo group have only been studied recently with respect to orbital interactions.[2,3] From the change in HOMO energy for a series of carbonyl containing diazomethanes, phenyldiazoacetophenone has been reported not to exhibit significant conjugation between phenyl and carbonyl π orbitals.[2] In a recent publication, we have confirmed this and have shown that the conformational behaviour of diazoacetophenone and a number of its para-substituted derivatives can be simulated accurately on the basis of Ph–C=O torsional potentials and orbital energy changes upon rotation of the phenyl ring.[3] The lack of π–π interaction in these compounds was attributed to the position of the carbonyl group: located between phenyl and diazo moieties, its low-lying orbitals lets it assume the role of an insulator.

We decided to perform studies on conformational and electronic structures of diazopropiophenone (**1**)

PII: S0040-4020(98)01182-X

(its PE spectrum[4] had been reported), its pyridinyl analogues **2a** and **2b** as well as their methyl diazoesters **3**, **4a**, and **4b** for several reasons: (*a*) compounds **2**, **3**, and **4** were available because of a planned PE spectroscopic pyrolysis study; (*b*) moving the diazo group closer to the aromatic ring in **3**, **4a**, and **4b** would remove the carbonyl's insulator capability which would allow for π–π interactions; and (*c*) this set of compounds offered an opportunity to elaborate on the electronic structure of the pyridinyl ring[5, 6] and determine its effect on orbital energies and conformational properties of diazoketones and diazoesters.

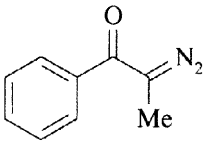

1

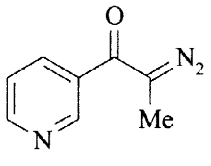

2a

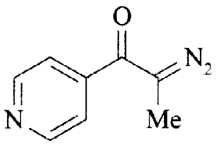

2b

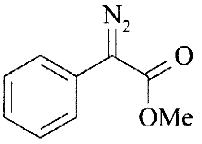

3

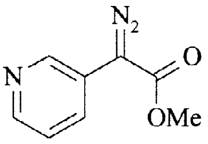

4a

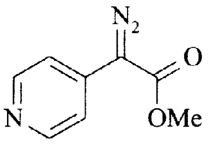

4b

EXPERIMENTAL

Ab initio HF[7] and Becke3LYP[8] calculations were carried out on IBM RS/6000 model 39H, 350, 530 and SP2 and SGI R10000 Impact computers with Gaussian 94.[9] Except for those dihedral angles fixed in torsional analyses and indicated in the text, all geometry parameters were optimized. Optimized geometries were shown to be minima by frequency calculations; total energies are uncorrected. Synthetic spectra were calculated from the MO results with a FORTRAN program PESPEC.[10] Ten eigenvalues (HOMO to HOMO−9, Becke3LYP/6-31+G*//Becke3LYP/6-31G*) were used to synthesize the partial PE spectra, convoluted with a Gaussian line shape with a full width at half height (FWHH) as indicated in the text and the temperature set at 300 K. Graphical representations of the computationally determined eigenvectors (Becke3LYP/6-31G*) were plotted from Chem3D.[11]

He(I) PE spectra were measured with a locally built instrument[12] by signal averaging 40–50 scans (10 scans in the case of **2a**, 20 scans for **3**). In order to achieve a suitable source pressure ($3–8 \cdot 10^{-3}$ Torr), samples were heated in bottle-shaped quartz vessels inserted into the tip of a heated probe (a maximum temperature of 80°C was used). Spectra were calibrated with the 15.6 eV band of nitrogen. Linearity of the scale was ensured through calibrations with methyl iodide (9.54 and 10.16 eV) and oxygen (12.30 eV) performed prior to the experiments. Vertical ionization potentials are accurate to ±0.05 eV.

Compounds **2**–**4** were synthesized by modification of standard procedures.[13]

RESULTS AND DISCUSSION

Calculated Conformational Properties

In a previous study on para-substituted diazoacetophenones (Ar–CO–C(N_2)H), AM1 potential energy surfaces obtained by varying N=C–C=O and phenyl–C=O dihedral angles from 0° to 180° revealed that diazoacetophenones prefer twisted synperiplanar *sp* (*syn*) rather than antiperiplanar *ap* (*anti*) conformations of the N=C–C=O group.[3] This behaviour was confirmed by *ab initio* HF/6-31G* calculations on *sp* and *ap* conformers. At this level of theory, the N=C–C=O twist angle for the unsubstituted species was found to be 2.2° and the phenyl ring was twisted against the carbonyl moiety by 17.0°; for the five para-substituted diazoacetophenones studied we received a uniform picture.

The results for diazoketones **1**, **2a**, and **2b** studied in this paper are similar to those mentioned above[14] with respect to *sp* and *ap* conformers of the N=C–C=O group. All *ap* conformers are less stable by about 12 kJ mol^{-1} at the semiempirical level (AM1 and PM3) and are not considered further (the terms *syn* and *anti* used for **2a** and **4a** during the rest of this paper are described below). As can be seen in Table 1, substitution of hydrogen on the carbon atom carrying the N_2 unit in the diazoacetophenones by the bulkier methyl group in diazoketones **1**, **2a**, and **2b** leads to an increase in both N=C–C=O and C=C–C=O dihedral angles: the twist in the diazoketo group it about three times that found in the diazoacetophenones, the twist of the aromatic ring against the carbonyl group is about twice as large. Values are similar for the three species at the two levels of theory applied. There is no such agreement for diazoesters **3**, **4a**, and **4b**. While HF/6-31G* data are

Table 1. Selected calculated dihedral angles (degrees) of diazoketones **1**, **2a**, and **2b** and diazoesters **3**, **4a**, and **4b**.

	HF/6-31G*		Becke3LYP/6-31G*	
	N=C–C=O	C=C–C=X	N=C–C=O	C=C–C=X
1	6.3	34.2	6.9	30.9
2a[a]	6.4	30.5	6.4	29.3
2b	5.0	38.1	5.6	32.9
3	1.5	38.7	2.4	25.3
4a[b]	0.7	43.6	2.0	23.2
4b	0.1	0.1	0.0	0.1

[a] For the *anti* conformer as shown in Fig. 1. [b] For the *syn* conformer as shown in Fig. 1.

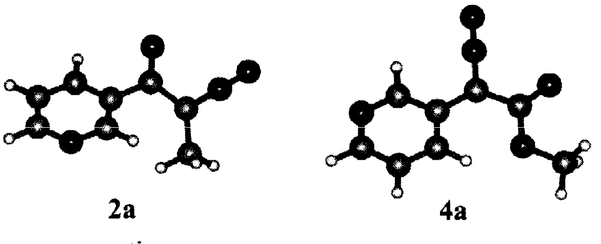
2a
anti
4a
syn

Fig. 1. *Anti* conformer of **2a** and *syn* conformer of **4a** (Becke3LYP/6-31G* geometries).

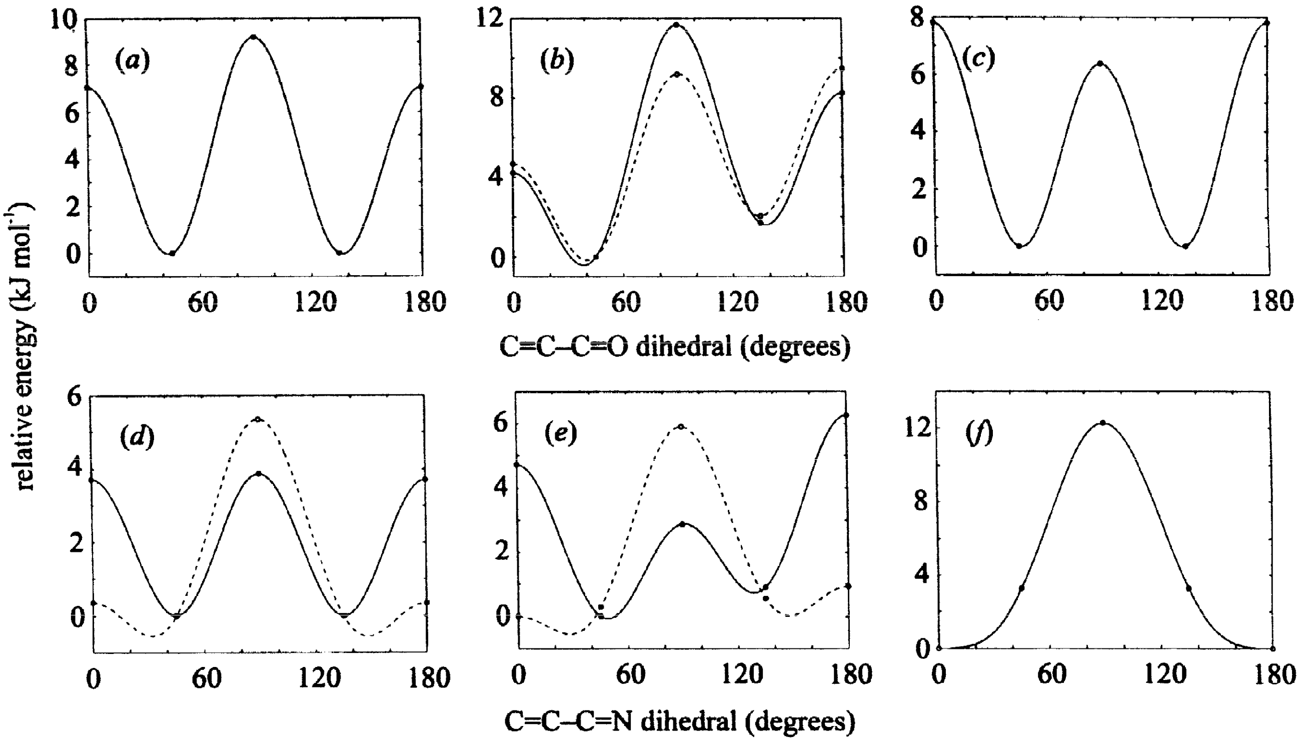

Fig. 2. Torsional potential calculated with PESPEC (HF/6-31G*, solid line; Becke3LYP/6-31+G*//HF/6-31G*, broken line): twist of the C=C–C=O dihedral of (*a*) **1**, (*b*) **2a**, and (*c*) **2b** and of the C=C–C=N dihedral of (*d*) **3**, (*e*) **4a**, and (*f*) **4b**.

dissimilar, according to Becke3LYP/6-31G* N=C–C=O and C=C–C=N torsional angles are considerably smaller than those for the diazoketones. This is most pronounced in **4b** which is found to be planar.

Introducing a nitrogen atom into the 3-position of the aromatic ring removes the symmetry of its 180° rotation and the degeneracy of the C=C–C=X rotamers in **2a** (X = O) and **4a** (X = N). This leads to two distinct conformers which we term *syn* and *anti* as given: pyridinyl nitrogen and carbonyl oxygen in **2a** (or diazo nitrogen in **4a**) atoms on the same side of an axis going through the pyridinyl–CX bond form a *syn* conformer; they are on different sides in an *anti* conformer (Fig. 1). Throughout the text, we refer to the more stable conformer of **2a** and **4a** as given in Fig. 1 (for total energies, see Table 2).

For the diazoacetophenones,[3] the highest energy species are those with the phenyl–C=O dihedral fixed at 90°. Torsional potentials – obtained by rotating the C=C–C=X dihedral through 180° in 45°-steps and relaxing the rest of the molecule – show that this is not necessarily the case for **1**–**4**. Fitted curves as calculated with PESPEC are given in Fig. 2. While potentials at the two levels of theory (HF/6-31G*, solid line; Becke3LYP/6-31+G*//HF/6-31G*, broken line) are fairly similar for **2a** (Fig. 2(*b*)) and virtually identical for **1**, **2b**, and **4b** (Figs. 2(*c*) and 2(*f*), respectively), we therefore only report the HF/6-31G* potential for **1**, **2b**,

Table 2. Total energies E_T (hartrees) of diazoketones **1**, **2a**, and **2b** and diazoesters **3**, **4a**, and **4b** (N electrons) and their radical cations[a] ($N-1$ electrons) as well as derived first vertical ionization potentials IP_v (eV).

	Number of electrons	HF/6-31G*	Becke3LYP/6-31G*	Becke3LYP/6-31+G*// Becke3LYP/6-31G*	
		E_T	E_T	E_T	IP_v
1	N	-529.172 377	-532.447 927	-532.468 860	8.51
	$N-1$			-532.156 060	
2a[b]	N	-545.165 093	-548.483 731	-548.505 220[c]	8.68
	$N-1$			-548.186 286	
2b	N	-545.162 975	-548.482 414	-548.504 012	8.77
	$N-1$			-548.181 881	
3	N	-604.047 313	-607.679 248	-607.702 847	7.98
	$N-1$			-607.409 622	
4a[d]	N	-620.039 610	-623.715 120	-623.739 116[e]	8.28
	$N-1$			-623.434 726	
4b	N	-620.041 396	-623.716 542	-623.740 800	8.53
	$N-1$			-623.427 481	

[a] Single point energy calculations on the optimized molecule (N electrons) geometries. [b] For the *anti* conformer as shown in Fig. 1. [c] E_T for the *syn* conformer is −548.482 589. [d] For the *syn* conformer as shown in Fig. 1. [e] E_T for the *anti* conformer is −623.714 794.

and **4b**, they are significantly different for diazoesters **3** and **4a** (Figs. 2(*d*) and 2(*e*), respectively).

Calculated Ionization Potentials, Molecular Orbitals and Orbital Energies

In previous publications, we have developed[15, 16] and successfully applied[3, 17] a routine for the interpretation of PE spectra based on Becke3LYP theory. This routine requires the calculation of the molecule's first vertical ionization potential IP_v which is determined from the energy difference between the neutral (N electrons, equilibrium geometry) and its radical cation ($N-1$ electrons, geometry of the neutral). Calculated orbital energies $-\varepsilon$ are then shifted uniformly so that the HOMO energy equals that of the IP_v, giving the higher *IP*s. While we have found the Becke3LYP/6-31+G* level of theory to serve us best in energy calculations in terms of performance versus computational requirements, geometry optimizations can be carried out at lower levels of theory; the concern about using orbital energies obtained with the HF/DFT hybrid method Becke3LYP has been commented on repeatedly.[3, 15-21] Total energies for **1**–**4**, their radical cations and derived IP_vs at the Becke3LYP/6-31+G*//Becke3LYP/6-31G* level are given in Table 2,

Table 3. Experimental and calculated vertical ionization potentials *IP* (eV) and orbital energies ε (eV) of diazoketones **1**, **2a**, and **2b** and diazoesters **3**, **4a**, and **4b**.

1	Becke3LYP[a]	$-\varepsilon$	6.53	7.06	7.38	7.48	9.77	10.06	10.18
		IP[b]	8.5	9.1	9.4	9.5	11.8	12.1	12.2
	exp.[c]	*IP*	8.52	9.1	--------9.5[d]-------				
2a	Becke3LYP[a]	$-\varepsilon$	6.71	7.25	7.64	7.86	8.36	10.46	10.83
		IP[b]	8.7	9.3	9.6	9.9	10.4	12.5	12.8
	exp.	*IP*	8.85	9.28	9.7	9.98	10.57	12.43	
2b	Becke3LYP[a]	$-\varepsilon$	6.82	7.37	7.60	7.76	8.35	10.31	10.84
		IP[b]	8.8	9.4	9.6	9.8	10.4	12.3	12.8
	exp.	*IP*	8.79	9.44	-------9.79[d]-------		10.57	12.43	
3	Becke3LYP[a]	$-\varepsilon$	6.20	7.27	7.97	8.21	8.69	9.69	9.96
		IP[b]	8.0	9.1	9.8	10.0	10.5	11.5	11.8
	exp.	*IP*	7.99	9.20	------10.10[d]------		10.79	11.57	
4a	Becke3LYP[a]	$-\varepsilon$	6.48	7.42	8.00	8.29	8.80	8.90	10.30
		IP[b]	8.3	9.2	9.8	10.1	10.6	10.7	12.1
	exp.	*IP*	8.42	9.53	9.98	10.3	10.79	11.06	12.51
4b	Becke3LYP[a]	$-\varepsilon$	6.71	7.35	7.55	8.40	9.00	9.07	10.10
		IP[b]	8.5	9.2	9.4	10.2	10.8	10.9	11.9
	exp.	*IP*	8.52	-------9.55[d]-------		10.53	11.00	11.14	12.39

[a] At the Becke3LYP/6-31+G*//Becke3LYP/6-31G* level of theory. [b] Orbital energies shifted uniformly, so that the HOMO energy[a] equals the calculated first IP_v as given in Table 2. [c] Taken from Ref. 4. [d] Consists of two overlapping bands.

orbital energies of the seven highest occupied MOs as well as *IP*s obtained from the shift are reported in Table 3.

As compounds **1**–**4** possess structural units with a multitude of electron lone pairs and π bonds, molecular orbitals composed of these are expected to give rise to the above calculated ionizations. For **1**, the highest occupied MOs consist of two π type orbitals (it is convenient to use the σ–π classification even though σ–π separation is lost in the non-planar compounds) from the phenyl ring as well as a $\pi_{C=N}$ and an n_O from the diazoketo group. These orbitals are also present in **2**–**4**, with an additional n_N from the pyridinyl nitrogen atom in **2a**, **2b**, **4a**, and **4b** and an $n_O(\pi)$ from the ester moiety in **3**, **4a**, and **4b**. While for diazoketones **1**, **2a**, and **2b** $\pi_{C=N}$ cannot mix with the ring π orbitals because of the low-lying $\pi_{C=O}$ of the carbonyl group which effectively functions as an insulator for $\pi_{C=N}$ and π MOs (as was found previously[2, 3] for diazoacetophenones), for diazoesters **3**, **4a**, and **4b** we find two orbitals with $\pi_{C=N}/\pi$ character that we term π^- (out of phase combination) and π^+ (in phase combination). MOs n_N and n_O, on the other hand, which are separate in **3**, **4a**,

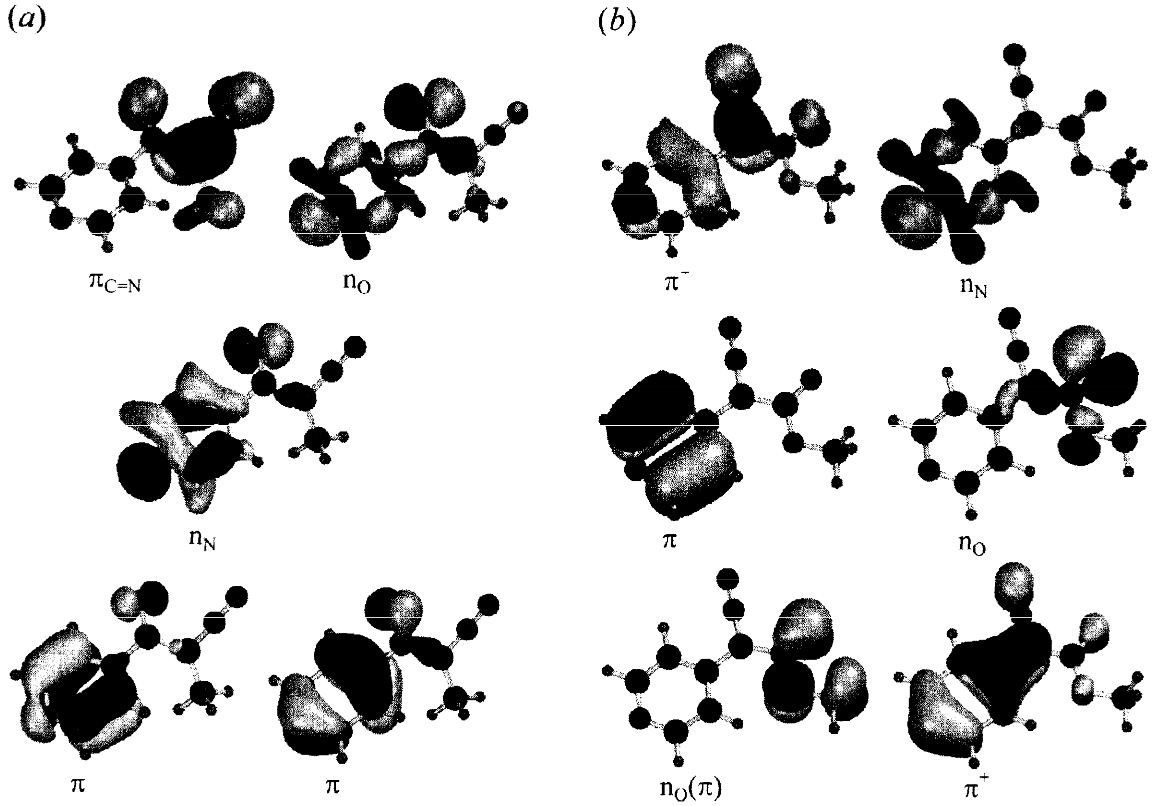

Fig. 3. (*a*) HOMO to HOMO−4 of diazoketone **2b** and (*b*) HOMO to HOMO−5 of diazoester **4b** (Becke3LYP/6-31G*).

and **4b**, mix in **1**, **2a**, and **2b**. Graphical representations of the MOs obtained at the Becke3LYP/6-31G* level are given in Fig. 3 for **2b** and **4b**; the eigenvectors were checked against those from Becke3LYP/6-31+G*//Becke3LYP/6-31G* calculations and were found to compare well. Even though there is "no physical relevance" to Kohn-Sham orbitals, in previous studies we have found eigenvectors obtained at the Becke3LYP/6-31+G* level of theory to be similar to those computed with HF/6-31G* or semiempirical PM3.[15,20,21] The orbital sequence in pyridine and its 4-methyl analogue is now accepted to be $n_N > \pi > \pi$[5b,c] and this is reproduced correctly with Becke3LYP theory; we also find the same order for 3-methylpyridine. From this and correlation diagrams based on calculated *IP*s as given in Table 3 we trust Becke3LYP/6-31+G*//Becke3LYP/6-31G* to give the correct order. Figures 4 and 5 each show a correlation diagram illustrating the influence of the pyridine nitrogen atom and of the switch in the heterobutadiene unit – on going from a diazoketone to a diazoester – on the calculated *IP*s as well as orbital assignments for **1**–**4**.

On going from **1** – the orbital sequence given in Fig. 4 is consistent with that in Ref. 4 – to **2** and from **3** to **4**, all levels are stabilized; ring π orbitals are affected more than other MOs according to the coefficient on the pyridinyl nitrogen atom. In pyridinyl compounds **2a** and **2b**, the order for ring MOs is n > π > π. The

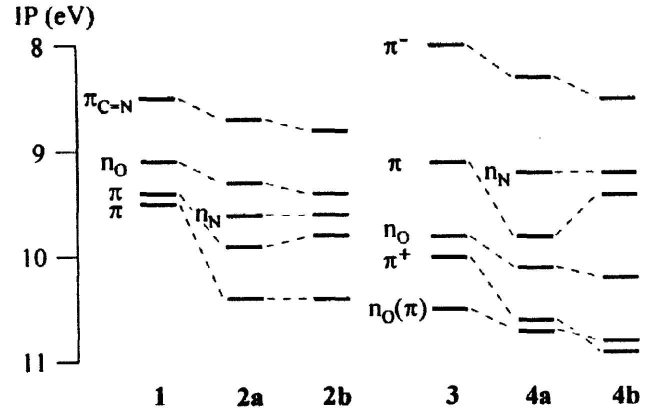

Fig. 4. Correlation diagram for **1**–**4**: going from a phenyl to a pyridinyl ring (Becke3LYP/6-31+G*//Becke3LYP/6-31G*).

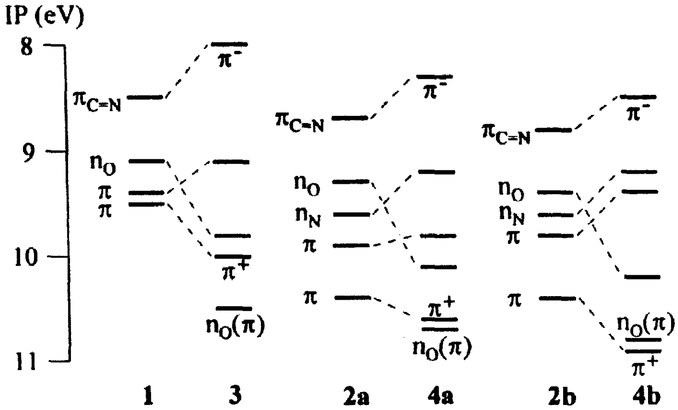

Fig. 5. Correlation diagram for **1**–**4**: going from a diazoketone to a diazoester (Becke3LYP/6-31+G*// Becke3LYP/6-31G*).

most striking feature in Fig. 4 is the destabilization of the HOMO−2 in **4b** with respect to **4a**. Because of the 3-position of the nitrogen in the ring and the energetic proximity of undisturbed π and $\pi_{C=N}$, the HOMO−2 of **4a** shows an unexpected orbital interaction. As the nitrogen atom is moved around the ring to the 4-position in **4b** this stabilizing interaction is lost and the HOMO−2 is raised in energy. Fig. 5 illustrates the extent of the π–π interaction in **3**, **4a**, and **4b** which becomes possible as the carbonyl group is moved from its insulating position in **1**, **2a**, and **2b**. Due to this interaction, π^- and π^+ in the diazoesters show a more pronounced splitting than is the case for the "original" levels of $\pi_{C=N}$ and π in the diazoketones; consequently the HOMO is found at significantly higher orbital energies (the first ionization at lower *IP*s). Interesting features in Fig. 5 are the changes in orbital energy of n_N and n_O. While these orbitals are separate in diazoesters **3**, **4a**, and **4b**, mixing of n_O on the more electronegative oxygen into n_N leads to a stabilization of the latter in the diazoketones; the opposite is true for mixing of n_N into n_O. Additionally, n_O in **3**, **4a**, and **4b**, having electron density on the C–O bond, is stabilized by the presence of the second oxygen atom.

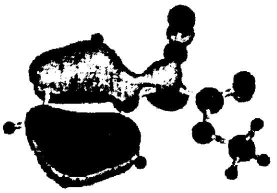

4a-HOMO-2

As for diazoacetophenones,[3] orbital energies of diazoketones **1**, **2a**, and **2b** show no significant dependence on the C=C–C=O torsional angle due to the lack of π–π interaction. Diazoesters **3**, **4a**, and **4b**, on the other hand, in which π type orbitals on the ring and the diazo moiety mix, show angular dependences of orbital energies as given in Fig. 6. Interpretation of the changes in orbital energies upon rotation of the ring is straightforward only for the HOMO which in all three cases is π^-. In the 90° conformation of **3**, the HOMO has lost its interaction and, as expected, is pure $\pi_{C=N}$. Yet the mirror image for the destabilization of HOMO−3 (π^+) which would lead to the pure π type orbital on the ring is not as pronounced as expected while the curve

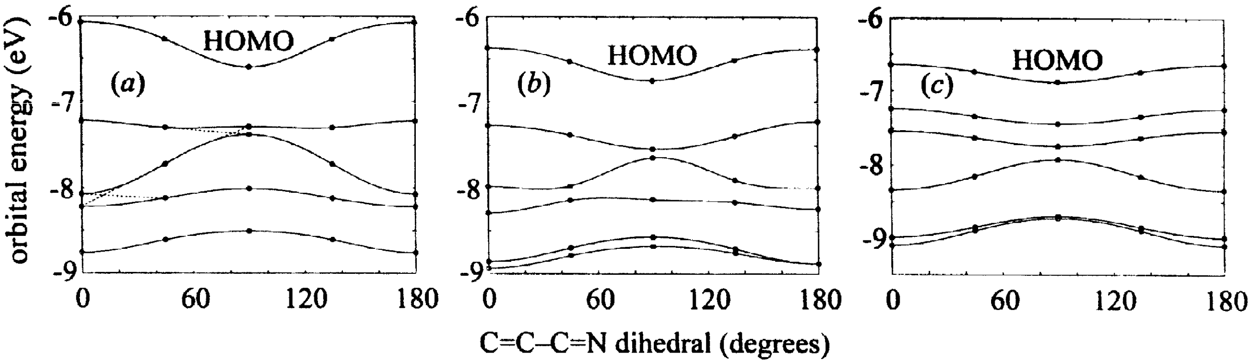

Fig. 6. Angular dependences of the MO energies of (*a*) HOMO to HOMO−4 of **3** as well as of HOMO to HOMO−5 of (*b*) **4a** and (*c*) **4b** (Becke3LYP/6-31+G*//Becke3LYP/6-31G*) obtained from PESPEC. Dashed lines in (*a*) indicate an avoided orbital crossing.

for HOMO−2 (n_O) shows this behaviour. An analysis of the eigenvectors in the 90° conformation (the orbital sequence is $\pi_{C=N} > \pi > \pi > n_O > n_O(\pi)$) clarifies the situation: the fitted curves show two avoided orbital crossings (as indicated in Fig. 6(*a*)), the 90° HOMO−1 being the π orbital allowed to interact with $\pi_{C=N}$ as the 90° dihedral is changed. Similar considerations apply for Figs. 6(*b*) and 6(*c*).

Experimental and Simulated Photoelectron Spectra

The He(I) photoelectron spectrum of **1** has been published,[4] those of **2**–**4** are depicted in Fig. 7, vertical ionization potentials for **1**–**4** are reported in Table 3. With five low-energy ionizations forming three bands (area ratio 1:3:1), spectra for diazoketones **2a** and **2b** are almost identical. They are similar to those of the respective acetylpyridines,[22] the ionization from the $\pi_{C=N}$ in **2a** and **2b** is simply added as first band which again demonstrates the lack of interaction between pyridinyl and diazoketo groups in the diazoketones. For **3**, there are four low-energy bands in front of the main group of σ bands corresponding to five ionizations. Spectra for diazoesters **4a** and **4b** differ in that for **4a** the six low-energy ionizations are grouped 1:1:2:2 (band area ratio) while for **4b** they are 1:2:1:2 due to the stabilization of the HOMO−2 in **4a** as explained above (Fig. 4).

The corresponding synthetic partial PE spectra – including deconvoluted bands – are given in Fig. 8. FWHHs of 0.4 were used for **1**, **2a**, and **2b**, 0.3 for **3**, and 0.6 for **4a** and **4b**. The simulations are based on the torsional potentials as given in Fig. 2 and use unshifted calculated MO energies. For **2a**, **3**, and **4a**, where potentials at the two levels of theory differ considerably, spectra were simulated using both potentials: for **3** and **4a**, the HF/6-31G* potentials were unable to reproduce the experimental spectra correctly and synthetic spectra for Becke3LYP/6-31+G*//HF/6-31G* surfaces are reported. When one takes into account the uniform

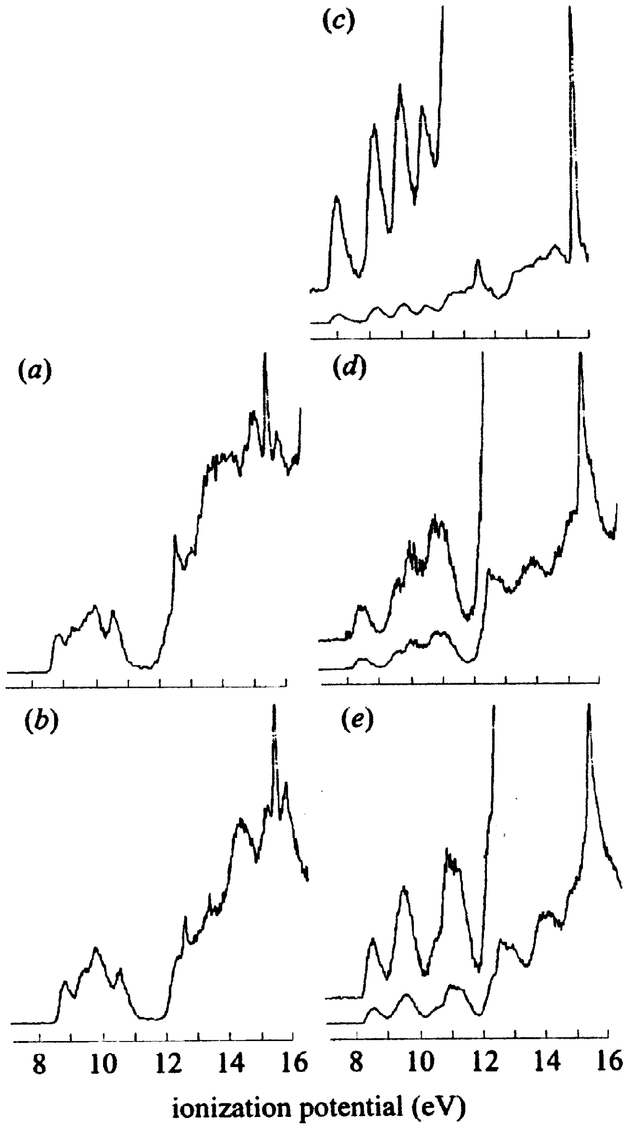

Fig. 7. He(I) photoelectron spectra of (*a*) **2a**, (*b*) **2b**, (*c*) **3**, (*d*) **4a**, and (*e*) **4b**.

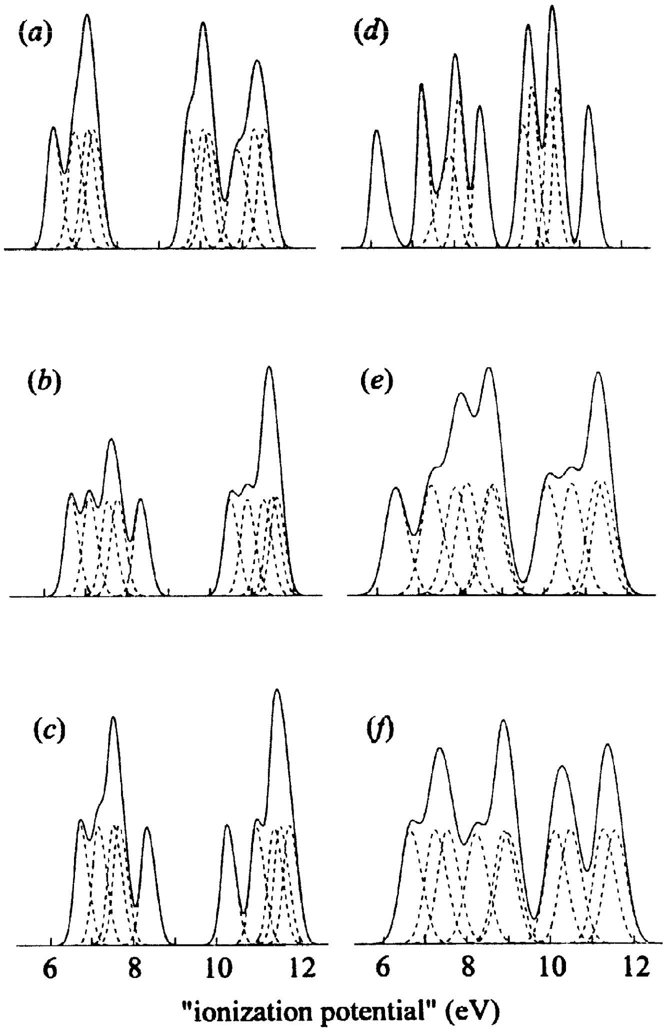

Fig. 8. Synthetic partial photoelectron spectra of (*a*) **1**, (*b*) **2a**, (*c*) **2b**, (*d*) **3**, (*e*) **4a**, and (*f*) **4b** from Becke3LYP/6-31+G*//Becke3LYP/6-31G* MO energies; (*a*), (*c*), and (*f*) use the HF/6-31G* surface, (*b*), (*d*), and (*e*) the Becke3LYP/6-31+G*//HF/6-31G* surface (Fig. 2).

shift that has to be applied to Becke3LYP MO energies (Table 3), a comparison between experimental and simulated spectra given reveals an awesome agreement, a fact that supports our interpretation of the electronic structure and conformational behaviour of these compounds.

CONCLUSION

We have recorded He(I) PE spectra of diazoketones **2** as well as diazoesters **3** and **4**, and interpreted the spectra of **1**–**4** with the aid of *ab initio* calculations. Calculated first vertical ionization potentials and uniformly shifted orbital energies at the Becke3LYP/6-31+G* level of theory match the experimental data almost perfectly. Correlation diagrams based on shifted orbital energies are able to explain changes in the appearance of the PE spectra. And finally, the quality of the synthesized PE spectra shows that the electronic structure of phenyl and pyridinyl diazoketones and diazoesters as a function of their conformational properties can be predicted accurately using Becke3LYP theory.

ACKNOWLEDGMENTS

We gratefully acknowledge the usage of the IBM SP2 computer at Queen's University granted under the auspices of an IBM Canada – Queen's University collaborative project as well as the usage of the SGI computing installation in the Geochemistry Labs at McMaster funded by NSERC. We thank Ms. O. Donini for assistance with operational aspects of parallel Gaussian 94 and the Natural Sciences and Engineering Research Council of Canada for financial support. We also thank Professor A.J. Kresge for a sample of phenyldiazo methyl acetate.

REFERENCES

1. For reviews, see Brown, R.S.; Jørgensen, F.S. In *Electron Spectroscopy: Theory, Techniques and Applications*; Vol. 5; Brundle, C.R.; Baker, A.D., Eds.; Academic Press; London, 1984. Klessinger, M.; Rademacher, P. *Angew. Chem. Int. Ed. Engl.* **1979**, *18*, 826.
2. Vorob'ev, A.S.; Furlei, I.I.; Ekov, Yu.Z.; Nazarov, A.M.; Yamilova, G.A.; Dzhemilev, U.M.; Dokichev, V.A. *Russ. Chem. Bull.* **1993**, *42*, 281.
3. Werstiuk, N.H.; Muchall, H.M.; Ma, J.; Liu, M.T.H. *Can. J. Chem.*, accepted.
4. Modelli, A; Innorta, G.; Torroni, S. *J. Electron Spectrosc. Relat. Phenom.* **1980**, *18*, 359.
5. For PE spectroscopic studies, see e.g. a) Kimura, K.; Katsumata, S.; Achiba, Y.; Yamazaki, T.; Iwata, S. *Handbook of HeI Photoelectron Spectra of Fundamental Organic Molecules*; Halsted Press; New York, 1981. b) Gleiter, R.; Heilbronner, E.; Hornung, V. *Angew. Chem. Int. Ed. Engl.* **1970**, *9*, 901. c) Heilbronner, E.; Hornung, V.; Pinkerton, F.H.; Thames, S.F. *Helv. Chim. Acta*, **1972**, *55*, 289. d) Moghaddam, M.S.; Bawagan, A.D.O.; Tan, K.H.; von Niessen, W. *Chem. Phys.* **1996**, *207*, 19.

6. For the performance of a number of semiempirical and *ab initio* methods on eigenvalues and eigenvectors of pyridine, see e.g. Danovich, D.K.; Turchaninov, V.K.; Zakrzewski, V.G. *J. Mol. Struct. (Theochem)*, **1990**, *209*, 77. Danovich, D.; Zakrzewski, V.; Domnina, E. *J. Mol. Struct. (Theochem)*, **1989**, *188*, 159. von Niessen, W.; Kraemer, W.P.; Diercksen, G.H.F. *Chem. Phys.* **1979**, *41*, 113 and references cited therein.
7. Hehre, W.J.; Radom, L.; Schleyer, P.v.R.; Pople, J.A. *Ab Initio Molecular Orbital Theory*; John Wiley & Sons; New York, 1986.
8. Becke, A.D. *J. Chem. Phys.* **1993**, *98*, 5648. Lee, C.; Yang, W.; Parr R.G. *Phys. Rev. B*, **1988**, *37*, 785.
9. Frisch, M.J.; Trucks, G.W.; Schlegel, H.B.; Gill, P.M.W.; Johnson, B.G.; Robb, M.A.; Cheeseman, J.R.; Keith, T.; Petersson, G.A.; Montgomery, J.A.; Raghavachari, K.; Al-Laham, M.A.; Zakrzewski, V.G.; Ortiz, J.V.; Foresman, J.B.; Peng, C.Y.; Ayala, P.Y.; Chen, W.; Wong, M.W.; Andres, J.L.; Replogle, E.S.; Gomperts, R.; Martin, R.L.; Fox, D.J.; Binkley, J.S.; Defrees, D.J.; Baker, J.; Stewart, J.P.; Head-Gordon, M.; Gonzalez, C.; Pople, J.A. *Gaussian 94*, Revision B.3; Gaussian, Inc.; Pittsburgh PA, 1995.
10. Werstiuk, N.H.; Timmins, G.; Ma, J.; Wildman, T.A. *Can. J. Chem.* **1992**, *70*, 1971.
11. CambridgeSoft Corporation; Cambridge, MA, USA, 1997.
12. Werstiuk, N.H.; Butler, D.N.; Shahid, E. *Can. J. Chem.* **1986**, *65*, 760.
13. Pitters, J.L.; Workentin, M.S., manuscript in preparation.
14. for CNDO/2 calculations on **1**, see Sorriso, S; Støgård, Å. *J. Chem. Soc. Perkin Trans. 2*, **1976**, 538.
15. Muchall, H.M.; Werstiuk, N.H.; Choudhury, B. *Can. J. Chem.* **1998**, *76*, 221.
16. Muchall, H.M.; Werstiuk, N.H.; Choudhury, B.; Ma, J.; Warkentin, J.; Pezacki, J.P. *Can. J. Chem.* **1998**, *76*, 238.
17. Muchall, H.M.; Rademacher, P. *J. Mol. Struct.*, in print.
18. Arduengo, A.J. III; Bock, H.; Chen, H.; Denk, M.; Dixon, D.A.; Green, J.C.; Herrmann, W.A.; Jones, N.L.; Wagner, M.; West, R. *J. Am. Chem. Soc.* **1994**, *116*, 6641.
19. Muchall, H.M.; Rademacher, P. *J. Mol. Struct.* **1997**, *435*, 157.
20. Werstiuk, N.H.; Muchall, H.M.; Roy, C.D.; Ma, J.; Brown, R.S. *Can. J. Chem.*, in print.
21. Muchall, H.M.; Werstiuk, N.H.; Ma, J.; Tidwell, T.T.; Sung, K. *Can. J. Chem.* **1997**, *75*, 1851.
22. Modelli, A.; Distefano, G. *J. Electron Spectrosc. Relat. Phenom.* **1981**, *23*, 323.